Substituent effect on the transition from ionic to covalent bonding in triphenylphosphonium ylide derivatives: reactivity of 3-methyl-2,2,2-triphenyl-2*H*-cyclohepta[*d*][1,2λ^5]oxaphosphole with heterocumulenes

Shin-ichi Naya and Makoto Nitta *

Department of Chemistry, School of Science and Engineering, Waseda University, Shinjuku-ku, Tokyo 169-8555, Japan

Received (in Cambridge, UK) 5th October 2001, Accepted 21st March 2002
First published as an Advance Article on the web 12th April 2002

X-Ray crystal analysis of 3-methyl-2,2,2-triphenyl-2*H*-cyclohepta[*d*][1,2λ^5]oxaphosphole [and the triphenylphosphonium ylide] **1a** and its parent compound **1b** has been carried out. The ^{31}P and ^{13}C NMR spectral studies of **1a**,**b** and their derivatives **1c**,**d**, and the correlation of their chemical shifts with P1–O1 bond lengths obtained by X-ray analyses for **1a**–**d** were investigated to clarify that compounds **1a**–**d** exist as resonance hybrids of a P–O bonding oxaphosphole structure (structure **A**) and a phosphonium ylide structure (structures **B** and **C**). The contribution of the structure **A** decreases gradually in the order of **1a** > **1c** > **1b** > **1d** in the solid state. On the basis of a linear correlation between P1–O1 bond lengths and θ_{sum} (the sum of bond angles between the equatorial bonds), it is clarified that an increase of the P1–O1 bonding character causes change in the configuration of the phosphorus atom from a tetrahedral to a trigonal bipyramidal arrangement. In connection with these studies, inspection of the structure of a related compound, 2,2,2-triphenyl-6,11-methano-2*H*-cycloundeca[*d*][1,2λ^5]oxaphosphole structure **2**, was also carried out. With a view to clarifying the reactivity of **1a** in connection with a contribution of canonical structures **A**, **B**, and **C**, compound **1a** was allowed to react with phenyl isocyanate, diphenylcarbodiimide, and phenyl isothiocyanate to give heteroazulenes. The reaction pathways depending on the contribution of canonical structures **A**, **B**, and **C** are discussed.

Introduction

Previously, Kawamoto and co-workers have reported structural studies[1,2] of triphenylphosphonium ylide derivatives **1c**,**d** (named as structures **B** and **C**) and reactivities[3,4] of **1a**–**c** (Scheme 1). The X-ray crystallographic analyses have revealed that compounds **1c**,**d** do not form a P–O bond, but there is appreciable coordinative interaction between the phosphorus and the oxygen atoms in the compounds. Thus, they have suggested that **1c**,**d** are regarded as "bonding betaines" which would be stabilized by a resonance hybrid between structures **A**, **B**, and **C**. On the other hand, we have reported recently the synthesis of 2-triphenylphosphoranylidenemethyl-5,10-methano[11]annulenone **2**, which exhibited a ^{31}P NMR signal at δ_P −36.3.[5] The pentacovalent phosphorus involved in a trigonal bipyramidal configuration exhibits ^{31}P NMR signals at δ_P −12 to −89, while the simple triphenylphosphonium ylide exhibits signals at δ_P 12 to 20.[6] Thus, compound **2** was considered to exist as the 2,2,2-triphenyl-6,11-methano-2*H*-cycloundeca[*d*]-[1,2λ^5]oxaphosphole structure **2**.[7] In addition, we have reported the synthesis of 2-(triphenylphosphoranylideneamino)tropone† **9** as the aza-analogue of **1b**.[8] Because of this connection, we have studied the thermal reactions of **1b**–**d**, **2**, and **9** with heterocumulenes **3**–**5** to obtain evidence for the P–O bonding structure and to explore a preparative method for annulated heterocycles (Scheme 2). Typical examples are as follows: the reaction of compound **2** with **3** afforded *N*-phenyl-6,11-methano-2*H*-cycloundeca[*b*]pyrrol-2-one **6**.[7] On the other hand, the reaction of **1b**–**d** with **3** gave 2*H*-cyclohepta[*b*]furan-2-ones **7b**–**d** along with *N*-phenyl-2*H*-cyclohepta[*b*]furan-2-imines **8b**–**d**.[7] Thus, the reaction pathways and the important contribution of a P–O bonding structure **A′** for **2**, as compared to that for **1b**–**d**, were clarified (Scheme 2). On the other hand, compounds **1a**,**b** reacted with dimethyl acetylenedicarboxylate or *N*-(4-methoxyphenyl)maleimide to give [8 + 2] and/or [4 + 2] cycloadducts, which retain an oxaphosphole skeleton.[4] In order to gain insight into the structures of **1a**–**d**, ^{31}P and ^{13}C NMR

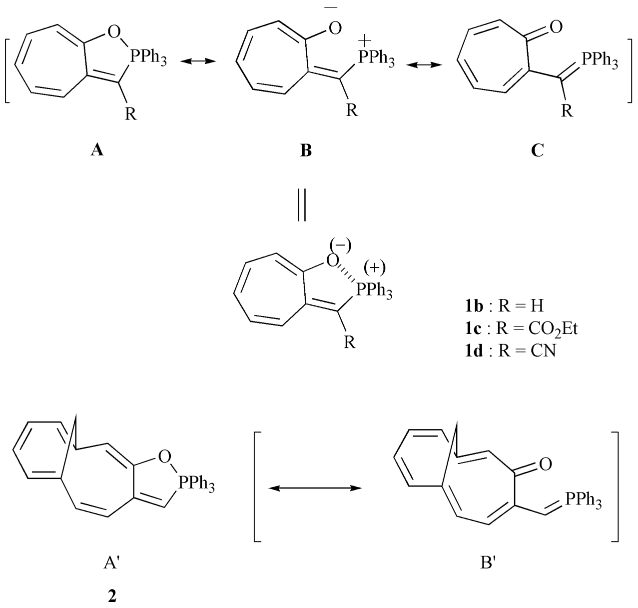

Scheme 1

---

† The IUPAC name for tropone is cycloheptatrienone.

DOI: 10.1039/b109076n

Table 1 ^{31}P NMR and ^{31}C NMR spectral data, and P1–O1, P1–C3 distance, and θ_{sum} obtained by X-ray structure analysis

	δ_P (CDCl$_3$)[a]		δ_P (solid)[a]	δ_C (CDCl$_3$)		X-Ray structure		
Compd.	rt	−60 °C	rt	C8a ($^2J_{P-O-C8a}$/Hz)	C3 ($^1J_{P-C3}$/Hz)	d(P1–O1)/Å	d(P1–C8)/Å	θ_{sum}/degree
1a	−17.9	−16.0	−22.1	170.1 (4.1)	87.0 (138)	2.00	1.79	355.4
1b	−3.6[b]	−1.8	−11.1	173.6 (4.1)	75.3 (143)	2.21	1.75	350.9
1c	−2.3[b]	−2.6	−14.3	176.6 (2.5)	73.3 (142)	2.14[c]	1.76[c]	352.8[c]
1d	+7.8[b]	+9.0	+2.8	177.5 (0.0)	49.4 (163)	2.36[d]	1.70[d]	347.0[d]

[a] The chemical shift is given relative to external 85% aqueous H_3PO_4 standard. [b] Ref. 7. [c] Ref. 1. [d] Ref. 2.

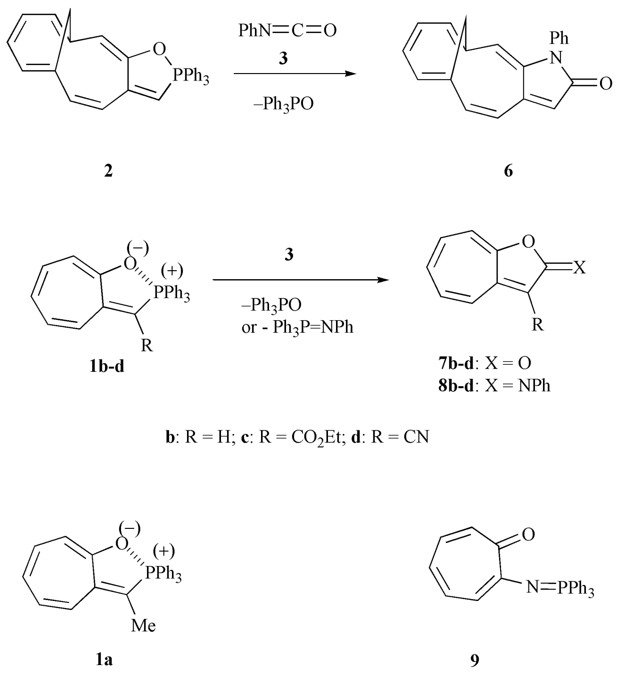

Scheme 2

spectroscopy and X-ray crystal analysis of **1a**,**b**, and reactions of **1a** with heterocumulenes were studied. On the basis of these studies, it was clarified that **1a**–**d** exist as resonance hybrids of structures **A**, **B**, and **C**, and the contribution of structure **A** decreases gradually in the order of **1a** > **1c** > **1b** > **1d**. Furthermore, an inspection of the structure of compound **2** was carried out. We describe herein the results in detail.

Results and discussion

Structure

The desired compound **1a** was prepared by the reaction of 2-chlorotropone with triphenylphosphonium ylide **11a** according to the modified procedure described in the literature (Scheme 3).[9] Compound **1b** was prepared similarly as described

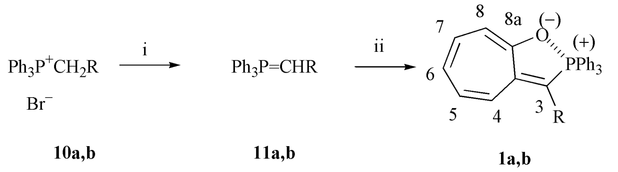

a: R = Me; **b**: R = H

Scheme 3 *Reagents and conditions*: i, rt, ^{t}BuOK, THF, 0.5 h; ii, 2-chlorotropone, rt, 2 h.

previously.[7,9] The detailed structures of compounds **1a**,**b** were confirmed by inspection of the spectroscopic data and X-ray structure analysis. Furthermore, inspection of the spectroscopic data of **1c**,**d** were also carried out in connection with the X-ray structure analyses reported in the literature.[1,2] The ^{31}P NMR spectral data in CDCl$_3$ at rt and −60 °C are summarized in Table 1. The ^{31}P NMR spectra of **1a**–**d** in CDCl$_3$ at rt exhibited signals at δ_P −17.9, −3.6, −2.3, and +7.8, respectively. The value for **1a** is comparable to that of pentacovalent phosphorus compounds having a trigonal bipyramidal structure (*vide supra*),[6] and it is lower than that of compound **2** (δ_P −36.3). The values for **1b**,**c** are lower than that for **1a**, and they are higher than that of simple triphenylphosphonium ylide.[6] The value of **1d** is close to that of simple triphenylphosphonium ylide.[6] These features suggest that **1a** has a large contribution of P–O bonding structure **A**, while **1d** has a large contribution of structures **B** and **C**. Furthermore, the structures of **1b**,**c** seem to have all the contributions of structures **A**, **B**, and **C**. The ^{31}P NMR spectra of **1a**–**d** in CDCl$_3$ at −60 °C exhibited signals at δ_P −16.0, −1.8, −2.6, and +9.0, respectively. Although these values are shifted to slightly lower-field compared with the corresponding values at rt, these signals show no splitting or broadening. This feature is completely different from that of 1,2λ^5-oxaphosphines **12a**–**f**, which exhibit two broad signals at δ_P −20 to −50 and +10 to +16 in CDCl$_3$ or benzene-d$_6$ possibly due to an equilibrium between **12a**–**f** and **13a**–**f**, respectively (Scheme 4).[10] Thus, these features suggest **1a**–**d** exist as resonance hybrids of **A**, **B**, and **C**, and are not in equilibrium between structures **A**, **B**, and **C**. The chemical shifts (δ_C) of C8a and C3 and their coupling constants between the carbon and phosphorus atoms in the ^{13}C NMR spectra of **1a**–**d** are also summarized in Table 1. The values for C8a of **1a**–**d** become lower in the order **1a** > **1b** > **1c** > **1d**, and the values for C3 become higher in the order **1a** < **1b** < **1c** < **1d**. These features are ascribed to the increase of the contribution of structures **B** and **C** in the order **1a** < **1b** < **1c** < **1d**: the increase of the contribution of structures **B** and **C** causes an increase in the positive charge of C8a and the negative charge of C3. The coupling constants between the carbon and phosphorus atoms also support the change in the contribution of structures **A**, **B**, and **C**. The increase of the contribution of structure **C** causes the increase of the P–C3 double bond character. Thus, coupling constant, $^1J_{P-C3}$, becomes larger in the order **1a** < **1b** < **1c** < **1d**. In a similar manner, the decrease of the contribution of structure **A** in the order **1a** > **1b** > **1c** > **1d** causes the decrease of the P–O bonding character. Thus, the coupling constant, $^2J_{P-O-C8a}$, becomes smaller in the order **1a** > **1b** > **1c** > **1d**. However, the coupling constants between the C8a and phosphorus atoms are considered to be generated by the P–C3–C3a–C8a coupling

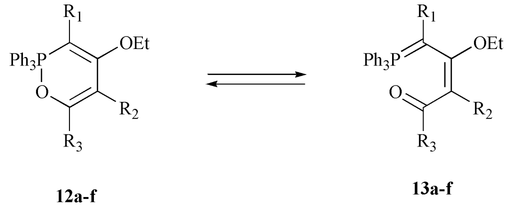

a: $R_1 = R_2 = H, R_3 = Ph$; **b**: $R_1 = R_2 = H, R_3 = OEt$
c: $R_1 = H, R_2 = Ph, R_3 = Ph$; **d**: $R_1 = H, R_2 = Ph, R_3 = OEt$
e: $R_1 = H, R_2 = Me, R_3 = Ph$; **f**: $R_1 = Me, R_2 = H, R_3 = Et$

Scheme 4

pathway as well as the P–O–C8a coupling pathway. Since the P–C3–C3a–C8a coupling pathway is coupling through three bonds, the effect of this pathway may be small. ^{31}P and ^{13}C NMR spectral data suggest that the contributions of structures **A**, **B**, and **C** become important in that order for **1a**–**d**.

The X-ray structure analyses of **1a**,**b** were examined. Selected bond lengths [*d*(P1–O1) and *d*(P1–C3)] and the sum of bond angles (θ_{sum}) are summarized in Table 1 along with those of **1c**,**d**.[12,13] The θ_{sum} value is defined by the sum of bond angles of the equatorial bonds, C8–P1–C10, C8–P1–C16, and C10–P1–C16, and the value correlates to a deviation from the planarity of the equatorial bonds (Fig. 3). Thus, the value of a typical tetrahedral configuration corresponds to 327.3°, and the sum of the equatorial bonds of a trigonal bipyramid adds up to 360°.[11] The X-ray structure analysis of **1a** suggested the existence of an appreciable electron density between the P1 and O1 atoms; thus, it is also suggested that the structure of **1a** has a large contribution of the P–O bonding structure **A**. The ORTEP drawings of compound **1a** and **1b** are shown in Fig. 1 and 2, respectively. Fig. 1 and 2 show that the phosphorus atom lies in a nearly trigonal bipyramidal configuration [(C22 and O1) are in apical positions; C8, C10, and C16 are in equatorial positions]. In compound **1a**, the angles of C8–P1–C16, C10–P1–C16, and C8–P1–C10 are 117.5, 116.4, and 121.5°, respectively, and the angles of C22–P1–O1, C22–P1–C8, C22–P1–C10, and C22–P1–C16 are 174.9, 99.9, 92.9, and 98.6°, respectively (Fig. 3). These values are similar to those of compound **1b**. The

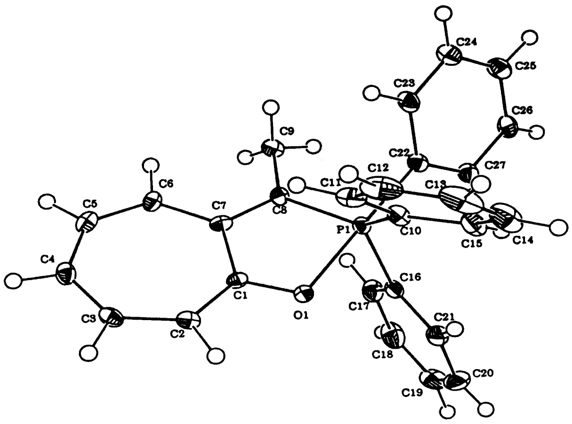

Fig. 1 An ORTEP drawing of **1a** with thermal ellipsoid plot (50% probability). Selected bond lengths (Å); P1–O1 1.999(3), P1–C8 1.785(4), P1–C10 1.822(4), P1–C16 1.825(4), P1–C22 1.871(4), O1–C1 1.293(5), C1–C2 1.392(5), C2–C3 1.403(6), C3–C4 1.372(6), C4–C5 1.404(6), C5–C6 1.362(6), C6–C7 1.426(5), C7–C8 1.390(5), C1–C7 1.476(5).

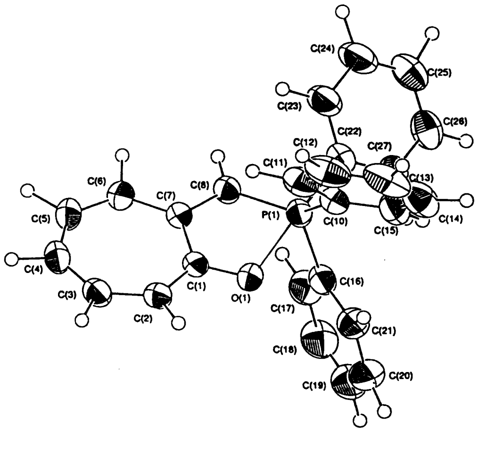

Fig. 2 An ORTEP drawing of **1b** with thermal ellipsoid plot (50% probability). Selected bond lengths (Å); P1–O1 2.2132(18), P1–C8 1.745(2), P1–C10 1.819(3), P1–C16 1.810(3), P1–C22 1.845(3), O1–C1 1.281(3), C1–C2 1.396(3), C2–C3 1.397(4), C3–C4 1.371(4), C4–C5 1.392(4), C5–C6 1.374(4), C6–C7 1.422(3), C7–C8 1.386(3), C1–C7 1.467(3).

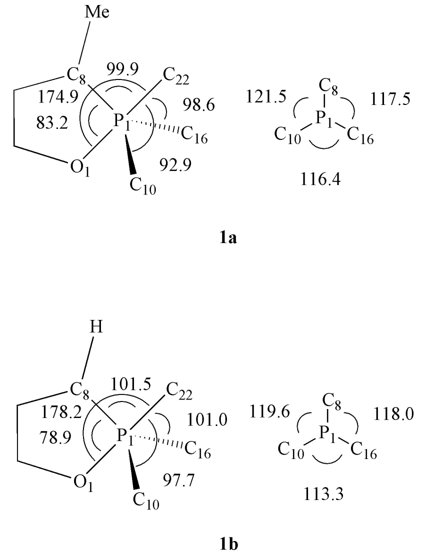

Fig. 3 Bond angles around the nearly trigonal bipyramidal structure of **1a** and **1b**.

P1–O1 bond lengths of **1a** (2.00 Å) and **1b** (2.21 Å) are larger than the typical P–O covalent bond in oxyphosphoranes (1.76–1.79 Å)[12] in bi- and tricyclic λ^5,σ^5-phosphoranes (1.63–1.65 Å),[13] or in 1,3,2λ^5-benzoxazaphosphole (1.88 Å),[14] but it is considerably shorter than the sum of the van der Waals radii (3.32 Å).[15] The value for **1a** is considerably shorter than those found in **1c** (2.14 Å)[1] and **1d** (2.36 Å),[2] while that of **1b** is longer than that of **1c** but shorter than that of **1d** (Table 1). Furthermore, the bond lengths of the C1–O1 bonds (1.29 Å for **1a** and 1.28 Å for **1b**) are longer than those found in **1c** (1.27 Å)[1] and **1d** (1.22 Å).[2] The seven-membered ring moieties in compounds **1a**,**b** are nearly planar, and the bond length alternations are clearly seen (1.36 and 1.48 Å for **1a** and 1.37 and 1.47 Å for **1b**); the result is in agreement with the evidence from the ^{1}H NMR spectra (Experimental section and ref. 7). The typical broad and strong carbonyl absorption of tropone[16] appearing at ν_{max} 1594 cm^{-1} is not observed in the IR spectra of **1a**,**b**, and the C1–O1 bond lengths (1.29, 1.28 Å) are longer than that of tropone (1.26 Å).[17]

In Fig. 4, P1–O1 bond lengths [*d*(P1–O1)] of **1a**–**d** were plotted against ^{31}P chemical shifts [δ_P(CDCl$_3$)] at rt. Except for **1c**, a linear correlation line was obtained, and the slope and

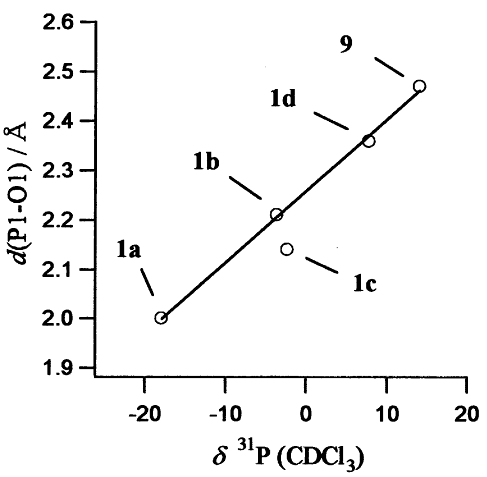

Fig. 4 Plot of P1–O1 bond length against ^{31}P chemical shift of **1a**–**d** and **9**.

y-intercept of this line were 0.0145 and 2.26, respectively, as expressed by eqn. (1) (correlation coefficient = 0.999). A plot of **9** (Scheme 2), which is an aza-analogue of **1b** [δ_P +14.1, d(P1–O1) 2.47 Å],[8] fits this regression line. Based on the X-ray structure analysis of **1c**, the oxygen atom of the ethoxy group is coordinated to the phosphorus atom.[2] Since the ethoxy group of **1c** rotates freely in solution, thus, a plot of **1c** evolves from this regression line. Therefore, the solid state ^{31}P MAS NMR of **1a**–**d** was measured (Table 1), and the P1–O1 bond lengths were plotted against the chemical shifts [δ_P(solid state)] in Fig. 5. A linear correlation line was obtained for **1a**–**d**, and the slope and y-intercept of this line were 0.0142 and 2.34, respectively, as expressed by eqn. (2) (correlation coefficient = 0.987). The plot of **1c** agrees with this regression line, and thus, the linear correlation between the ^{31}P chemical shifts and the P1–O1 distance is confirmed. Based on eqn. (1), the P1–O1 bond length of **2** (^{31}P δ_P −36.3) is estimated to be 1.73 Å. The value corresponds to the typical P–O covalent bond in oxyphosphoranes (1.76–1.79 Å).[12] Thus, the structure of **2** is considered to have a large contribution of P–O bonding structure **A′** as compared with that of structure **B′** (Scheme 1). Moreover, P1–C3 bond lengths [d(P1–C3)] of **1a**–**d** were plotted against P1–O1 bond lengths (Fig. 6) as expressed by eqn. (3) (correlation coefficient = 0.998).

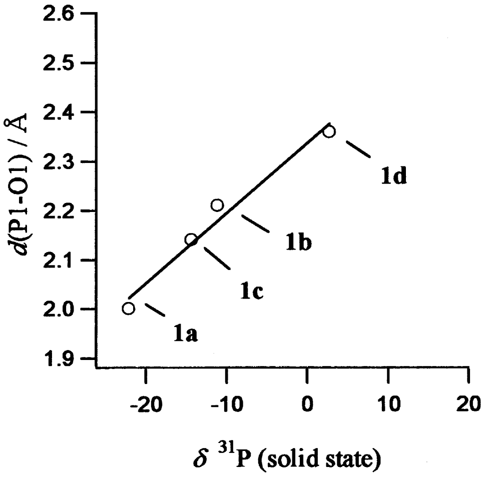

Fig. 5 Plot of P1–O1 bond length against ^{31}P chemical shift of **1a**–**d**.

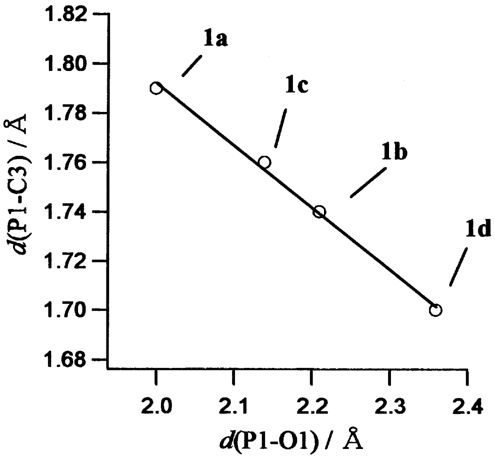

Fig. 6 Plot of P1–C3 bond length against P1–O1 bond length of **1a**–**d**.

A linear correlation line was also obtained, and the slope and y-intercept of this line were −0.252 and 2.30, respectively. These features show that the contribution of structure **A** decreases gradually in the order **1a** > **1c** > **1b** > **1d** in the solid state. On the other hand, θ_{sum} values were plotted against P1–O1 bond lengths (Fig. 7). A linear correlation line was obtained, and the slope and y-intercept of this line were −23.2 and 402.1, respectively, as expressed by eqn. (4) (correlation coefficient = 0.995). This feature shows that coordination of the oxygen atom to the phosphorus atom causes a change in the phosphorus atom from tetrahedral configuration to trigonal bipyramidal configuration. Based on eqn. (4) and the calculated P1–O1 bond length of **2** (1.73 Å, *vide supra*), θ_{sum} of **2** is calculated to be 362°. This value agrees with the trigonal bipyramidal configuration of the phosphorus atom of **2**, which is also considered to have a large contribution of P–O bonding structure **A′** (Scheme 1). Based on this value and eqn. (4), the P1–O1 bond length is calculated to be 3.22 Å when the phosphorus atom changes to a tetrahedral configuration (θ_{sum} = 327.3°; *vide supra*). This bond length is close to the sum of the van der Waals radii (3.32 Å).[15] Thus, disappearance of interaction between the oxygen and phosphorus atoms favors a tetrahedral configuration of the phosphorus atom, and thus, the compound becomes simple triphenylphosphonium ylide **11b**.

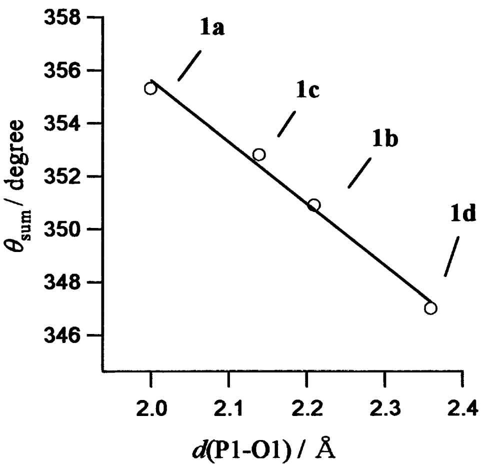

Fig. 7 Plot of θ_{sum} against P1–O1 bond length of **1a**–**d**.

$$[d(\mathrm{P1{-}O1})] = 0.0145[\delta_P(\mathrm{CDCl_3})] + 2.26 \quad (1)$$

$$[d(\mathrm{P1{-}O1})] = 0.0142[\delta_P(\text{solid state})] + 2.34 \quad (2)$$

$$[d(\mathrm{P1{-}O3})] = -0.252[d(\mathrm{P1{-}O1})] + 2.30 \quad (3)$$

$$[\theta_{sum}] = -23.2\ [d(\mathrm{P1{-}O1}) + 402.1 \quad (4)$$

Reactivity

Reactions of oxaphosphole **1a** with heterocumulenes were carried out first. Compound **1a** reacted with phenyl isocyanate **3** to give 3-methyl-2*H*-cyclohepta[*b*]furan-2-one **7a**,[18] its imine derivative **8a**, and *N*-phenyl-3-methylcyclohepta[*b*]pyrrol-2-one **14** in good combined yield. Similarly, the reaction of **1a** with diphenylcarbodiimide **4** gave only **8a** in modest yield. On the other hand, the reaction of **1a** with phenyl isothiocyanate **5** afforded *N*-phenyl-3-methyl-2*H*-cyclohepta[*b*]pyrrole-2-thione **15** and 3-methyl-2-(*N*-phenylamino)-4*H*-cyclohepta[*b*]thiophen-4-one **16** in moderate yield (Scheme 5). The reaction conditions and the yields of products are summarized in Table 2. The structures of new compounds **8a**, and **14**–**16** were unequivocally assigned on the basis of their ^{1}H and ^{13}C NMR spectra, IR spectra, and mass spectral data, as well as analytical data and/or HRMS data. The ^{1}H NMR and IR spectra of **8a**, and **14** are similar to those of the compounds having no methyl group.[7] The IR spectrum of compound **15** exhibits typical absorption due to the thioamide function.[7,19] The ^{1}H NMR and IR spectra of **16** are similar to those of 4*H*-cyclohepta[*b*]thiophen-4-one[20] and 2-(*N*-phenylamino)-4*H*-cyclohepta[*b*]thiophen-4-one.[7] The yield of **8a** is low, and satisfactory analytical data are not obtained; but the HRMS data are satisfactory. Furthermore,

Table 2 Reaction of **1a** with heterocumulenes **3**–**5**

Entry	Heterocumulene	**3**–**5** : **1a** ratio	Reaction conditions[a]		Product [yield (%)][b]
			Solvent	Time/h	
1	**3**	2.0	Dioxane	9	**7a** (76), **8a** (2), **14** (22)
2	**4**	2.0	Anisole	12	**8a** (13)
3	**5**	2.0	Dioxane	2	**15** (23), **16** (41)

[a] Reactions were carried out under reflux. [b] Yields are based on **1a**.

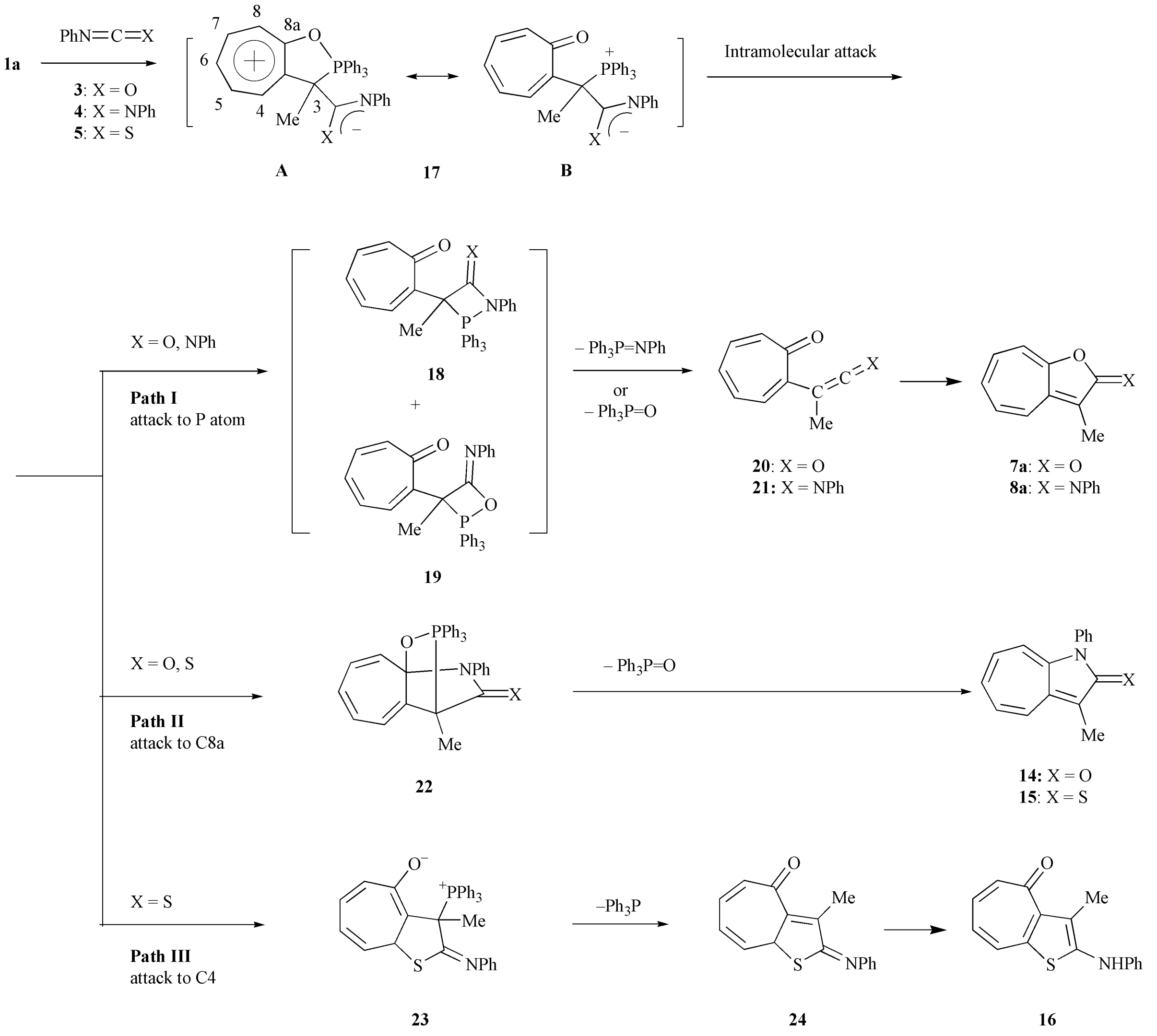

Scheme 5

compound **8a** is not a mixture of (*E*)- and (*Z*)-isomers. Although no evidence for the stereochemical situation for **8a** is obtained, we suspect the (*Z*)-isomer for **8a**, because of the steric hindrance of the methyl group.

We propose the pathways for the formation of the products **7a**, **8a**, and **14**–**16** as outlined in Scheme 5. Addition of C3 of **1a** to the carbonyl carbon atom of **3**–**5**, as in the case of the reaction of **1b**–**d** and **2** with **3** and **5**,[7] gives rise to the intermediate **17** (X = O, NPh, and S). The P–O bond cleavage in **17** (X = O, NPh) seems to be the predominant pathway (Path I) to give the intermediate **18** and **19**. The intermediates **18** and **19** undergo elimination of Ph$_3$PO or Ph$_3$PNPh to result in the formation of **7a** and **8a**, respectively. This process has been found as the only pathway proposed for the reaction of **1b**–**d** with **3** and **4**.[7] On the other hand, the intermediate **17** (X = O and X = S) undergoes intramolecular addition (Path II) to give the intermediate **22**, which eliminates Ph$_3$PO to result in the formation of cycloheptapyrroles **14** and **15**. In addition, the intermediate **17** (X = S) involves a sulfide ion having soft nucleophilicity, and it also undergoes intramolecular nucleophilic attack (Path III) to give the intermediate **23**, which eliminates Ph$_3$P and undergoes aromatization to give thiophene derivative **16**.[7] The formation of **14**–**16** is considered to be chemical evidence for the large contribution of structure **A** in **1a**, as in the case of the reaction of **2** with heterocumulenes **3** and **5**.[7] The formation of **14**–**16** shows that intramolecular nucleophilic attack on the seven-membered ring occurred in the intermediate **17**, in which the positive charge is delocalized to the seven-membered ring. Thus, a contribution of P–O bonding structure **17-A** is considered to be important in the intermediate **17**. In addition, intramolecular nucleophilic attack on C8a in Path II suggests that the intermediate **17** has a large contribution of P–O bonding structure **17-A**. On the basis of the AM1 calculation (MOPAC97),[21] the carbonyl carbon atom of tropone has no coefficient in the LUMO (*cf.* **17-B**); thus, the nucleophilic attack on the carbonyl carbon atom seems to be unlikely. On the contrary, the *ipso*-carbon atom of the substituted tropylium ion has a large coefficient in the LUMO. Therefore, a large contribution of P–O bonding structure **17-A** in the intermediate **17** favors the intramolecular nucleophilic attack on C8a.

In summary, the ^{31}P and ^{13}C NMR spectral studies and the X-ray crystallographic analysis revealed that **1a**–**d** exist as resonance hybrids of canonical structures **A**, **B**, and **C**. A linear correlation between ^{31}P chemical shifts and P1–O1 bond lengths is obtained. The contribution of canonical structure **A** decreases gradually in the order of **1a** > **1c** > **1b** > **1d** in the solid state. On the basis of a linear correlation between P1–O1 bond lengths and θ_{sum}, it is clarified that the increase in P1–O1 bonding character causes a change in configuration of the phosphorus atom from a tetrahedral to a trigonal bipyramidal arrangement. On the basis of the study, the structure of **2** is confirmed as well. On the other hand, the electron-donating methyl group makes **1a** have a large contribution of P–O bonding structure **A**. On the contrary, the electron-withdrawing nitrile group generally stabilizes ylides, and thus, **1d** has a large contribution of canonical structures **B** and **C**. It is established that reactions of **1a** with heterocumulenes give not only products arising from a contribution of structure **A** but also products derived from structures **B** and **C**. The reaction provides a methodology for constructing new derivatives of heteroazulenes.

Experimental

IR spectra were recorded on a Perkin-Elmer 1640 spectrometer. Mass spectra and high-resolution mass spectra were run on JMS-AUTOMASS 150 and JMS-SX102A spectrometers. ^{1}H NMR spectra and ^{13}C NMR spectra were recorded on JNM-AL300, JNM-GSX400, and JNM-LA500 spectrometers using $CDCl_3$ as a solvent, and the chemical shifts are given relative to internal $SiMe_4$ standard; *J*-values are given in Hz. ^{31}P NMR (109.3 MHz) spectra were recorded on a JNM-EX270 spectrometer, and the chemical shifts are given relative to external aqueous 85% H_3PO_4 standard (the negative value denotes signals appearing at higher field than the standard). The solid state ^{31}P MAS NMR (161.8 MHz) spectra were recorded on a JNM-GSX400 spectrometer, and the chemical shifts are given relative to external aqueous 85% H_3PO_4 standard (the negative value denotes signals appearing at higher field than the standard). Microanalysis was performed at the Materials Characterization Central Laboratory, Waseda University. Mps were recorded on a Yamato MP-21 apparatus and are uncorrected. All the reactions were carried out under anhydrous conditions and dry nitrogen atmosphere. Dioxane refers to 1,4-dioxane throughout.

Preparation of 3-methyl-2,2,2-triphenyl-2*H*-cyclohepta[*d*][1,2λ^5]-oxaphosphole 1a

A solution of ethyltriphenylphosphonium bromide (11.13 g, 30 mmol) and *tert*-BuOK (3.36 g, 30 mmol) in THF (30 cm^3) was stirred at rt for 0.5 h. To the solution was added 2-chlorotropone (2.11 g, 15 mmol), and the mixture was stirred for 2 h at rt. After the THF was removed *in vacuo*, the resulting residue was dissolved in CH_2Cl_2 and filtered to remove insoluble materials. The filtrate was concentrated and the residue was chromatographed on Al_2O_3 using hexane–AcOEt (1 : 1) as the eluent to give **1a** (3.46 g, 59%).

For 1a. Reddish plates; mp 208–209 °C (from EtOH) (lit.[9] 212–213 °C); δ_H (500 MHz) 1.44 (3H, d, J_{HP} 17.6, Me), 5.82 (1H, d, *J* 10.0, H-8), 6.05 (1H, dd, *J* 10.1, 9.6, H-6), 6.56 (1H, dd, *J* 10.1, 10.0, H-7), 6.69 (1H, dd, *J* 11.3, 9.6, H-5), 6.72 (1H, d, *J* 11.3, H-4), 7.20–7.60 (15H, br s, Ph); ν_{max} ($CHCl_3$)/cm^{-1} 1598, 1564, 1504.

Reaction of 1a with phenyl isocyanate 3

A solution of **1a** (197 mg, 0.5 mmol) and **3** (119 mg, 1 mmol) in dioxane (2 cm^3) was heated under reflux for 9 h. The reaction mixture was concentrated and the residue was chromatographed on SiO_2. The fractions eluted with hexane–AcOEt (1 : 1) were concentrated, and the resulting residue was separated by TLC on SiO_2 (hexane–AcOEt: 2 : 1) to give **7a**, **8a**, and **14**. Results are summarized in Table 2.

For 7a. Orange plates; mp 108–109 °C (from EtOH) (lit.[18] 105–106 °C); δ_H (500 MHz) 2.02 (3H, s, Me), 6.67 (1H, dd, *J* 11.0, 8.4, H-6), 6.77 (1H, d, *J* 9.0, H-8), 6.84 (1H, dd, *J* 11.0, 9.0, H-7), 6.91 (1H, dd, *J* 11.4, 8.4, H-5), 7.08 (1H, d, *J* 11.4, H-4); δ_C (125.6 MHz) 7.8, 108.0, 111.8, 126.2, 129.4, 131.8, 133.7, 147.4, 157.6, 170.2; ν_{max} ($CHCl_3$)/cm^{-1} 1745, 1271; *m*/*z* (rel. int.) 160 (M$^+$, 33%), 131 (100) (Found: C, 75.1; H, 4.9. $C_{10}H_8O_2$ requires C, 74.99; H, 5.03%).

For 8a. Red needles; mp 134–135 °C (from EtOH); δ_H (500 MHz) 2.01 (3H, s, Me), 6.13 (1H, d, *J* 8.8, H-8), 6.14 (1H, dd, *J* 11.4, 8.1, H-6), 6.35 (1H, dd, *J* 11.4, 8.8, H-7), 6.42 (1H, dd, *J* 11.6, 8.1, H-5), 6.67 (1H, d, *J* 11.6, H-4), 7.08 (1H, t, *J* 7.2, *p*-Ph), 7.26 (2H, d, *J* 8.4, *o*-Ph), 7.32 (2H, dd, *J* 8.4, 7.2, *m*-Ph); δ_C (125.6 MHz) 8.4, 107.0, 115.7, 123.4, 123.7, 125.5, 127.2, 128.7, 131.3, 132.1, 142.0, 146.6, 158.9, 161.5; ν_{max} ($CHCl_3$)/cm^{-1} 1659, 1267; *m*/*z* (rel. int.) 235 (M$^+$, 75%), 77 (100) (HRMS: Found: M$^+$ + 1, 236.1075. $C_{22}H_{16}O$ requires M$^+$ + 1, 236.1059).

For 14. Orange needles; mp 184–185 °C (from EtOH); δ_H (500 MHz) 2.20 (3H, s, Me), 6.59 (1H, d, *J* 9.0, H-8), 6.72 (1H, dd, *J* 11.0, 8.4, H-6), 6.82 (1H, dd, *J* 11.0, 9.0, H-7), 6.94 (1H, dd, *J* 11.4, 8.4, H-5), 7.33 (2H, d, *J* 8.4, *o*-Ph), 7.39 (1H, d, *J* 11.4, H-4), 7.46 (1H, t, *J* 7.5, *p*-Ph), 7.54 (2H, dd, *J* 8.4, 7.5, *m*-Ph); δ_C (125.6 MHz) 8.1, 111.2, 111.9, 126.7, 128.1, 128.5, 128.6, 129.4, 130.1, 130.4, 134.6, 140.4, 145.3, 169.2; ν_{max} ($CHCl_3$)/cm^{-1} 1667; *m*/*z* (rel. int.) 235 (M$^+$, 83%), 77 (100) (Found: C, 81.4; H, 5.5; N, 5.9. $C_{16}H_{13}NO$ requires C, 81.68; H, 5.57; N, 5.95%).

Reaction of 1a with diphenylcarbodiimide 4

A solution of **1a** (99 mg, 0.25 mmol) and **4** (97 mg, 0.5 mmol) in anisole (5 cm^3) was heated under reflux for 12 h. The reaction mixture was then separated by TLC on SiO_2 (hexane–AcOEt: 3 : 1) to give **8a**. The results are summarized in Table 2. The physical data are identical with those of the authentic specimen.

Reaction of 1a with phenyl isothiocyanate 5

A solution of **1a** (197 mg, 1 mmol) and **5** (270 mg, 2 mmol) in dioxane (3 cm^3) was heated under reflux for 2 h. The reaction mixture was concentrated and the residue was chromatographed on SiO_2. The fractions eluted with hexane–AcOEt (1 : 1) were concentrated and the residue was separated by TLC on SiO_2 (hexane–AcOEt: 1 : 1) to give **15** and **16**. Results are summarized in Table 2.

For 15. Dark green plates; mp 108–109 °C (from EtOH); δ_H (500 MHz) 2.44 (3H, s, Me), 6.72–6.77 (1H, m, H-8), 6.96–7.05 (2H, m, H-6, 7), 7.15–7.19 (1H, m, H-5), 7.32 (2H, d, *J* 8.6, *o*-Ph), 7.55 (1H, t, *J* 7.3, *p*-Ph), 7.58–7.62 (3H, m, *m*-Ph, H-4); δ_C (125.6 MHz) 10.7, 115.1, 125.3, 128.2, 129.2, 129.3, 129.6, 131.1, 131.4, 131.5, 136.7, 139.1, 149.5, 187.8; ν_{max} ($CHCl_3$)/cm^{-1} 1577, 1542, 1495, 1427, 1383, 1372, 1330, 1270, 1070, 1024; *m*/*z* (rel. int.) 251 (M$^+$, 33%), 77 (100) (Found: C, 76.6; H, 5.5; N, 5.6. $C_{16}H_{13}NS$ requires C, 76.46; H, 5.21; N, 5.57%).

For 16. Orange needles; mp 153–154 °C (from EtOH); δ_H (500 MHz) 2.55 (3H, s, Me), 5.89 (1H, s, NH), 6.63 (1H, dd, *J* 11.0, 8.1, H-7), 6.94 (1H, d, *J* 12.1, H-5), 6.99 (1H, t, *J* 7.3, *p*-Ph), 7.02 (1H, dd, *J* 12.1, 8.1, H-6), 7.03 (2H, d, *J* 8.6, *o*-Ph), 7.27 (1H, d, *J* 11.0, H-8), 7.30 (2H, dd, *J* 8.6, 7.3, *m*-Ph); δ_C (125.6 MHz) 14.2, 116.4, 121.9, 124.1, 128.6, 129.6, 130.4, 133.8, 137.4, 139.4, 143.9, 145.9, 184.0; ν_{max} ($CHCl_3$)/cm^{-1} 3413, 1579, 1497, 1445, 1391; *m*/*z* 267 (M^+, 9%), 77 (100) (Found: C, 72.2; H, 4.7; N, 5.2. $C_{16}H_{13}NOS$ requires C, 71.86; H, 4.90; N, 5.24%).

X-Ray structure determination ‡

For 1a. Red prisms, $C_{27}H_{23}OP$, $M = 394.45$, orthorhombic, space group *Pbca*, $a = 17.5193(4)$, $b = 13.2112(8)$, $c = 17.8502(5)$ Å, $V = 4131.4(2)$ Å^3, $Z = 8$, $D_c = 1.268$ g cm^{-3}, crystal dimensions 0.50 × 0.20 × 0.20 mm. Data were measured on a Rigaku RAXIS-RAPID radiation diffractomater with graphite monochromated Mo-Kα radiation. A total 39328 reflections were collected, using the $\omega - 2\theta$ scan technique to a maximum 2θ value of 55.0°. The structure was solved by direct methods and refined by a full-matrix least-squares method using SIR92 structure analysis software,[22] with 354 variables and 3539 observed reflections [$I > 3.00\sigma(I)$]. The non-hydrogen atoms were refined anisotropically. The weighting scheme $w = [\sigma_c^2(F_0) + 0.010 \times F_0^2]^{-1}$ gave satisfactory agreement analysis. The final *R* and *Rw* values were 0.069 and 0.142. The maximum peak and minimum peak in the final difference map were 0.75 and −0.67 e Å^{-3}.

For 1b. Orange prisms, $C_{26}H_{21}OP$, $M = 380.43$, orthorhombic, space group *Pbca*, $a = 17.54$, $b = 17.50$, $c = 13.35$ Å, $V = 4095.59$ Å^3, $Z = 8$, $D_c = 1.234$ g cm^{-3}, crystal dimensions 0.20 × 0.20 × 0.20 mm. Data were measured on a MAC Science MXC radiation diffractomater with graphite monochromated Cu-Kα radiation. A total 4529 reflections were collected, using the $\omega - 2\theta$ scan technique to a maximum 2θ value of 139.98°. The structure was solved by direct methods and refined by a full-matrix least-squares method using SHELXL-97 structure analysis software, with 253 variables and 3689 observed reflections [$I > 3.00\sigma(I)$]. The non-hydrogen atoms were refined anisotropically. The weighting scheme $w = [\sigma_c^2(F_0) + (0.1033 \times P)^2 + 3.0000 \times P]^{-1}$ gave satisfactory agreement analysis [$P = (F_0^2 + 2Fc^2)/3$]. The final *R* and *Rw* values were 0.064 and 0.177.

---

‡ CCDC reference numbers 172471 and 172472. See http://www.rsc.org/suppdata/p2/b1/b109076n/ for crystallographic files in .cif or other electronic format.

Acknowledgements

Financial support from a Waseda University Grant for a Special Research Project is gratefully acknowledged. The authors thank Analytical Chemistry Laboratories, Central Research Laboratories, Ajinomoto Co., Inc., for the X-ray structure analysis. The authors also thank the Materials Characterization Central Laboratory, Waseda University, for technical assistance with the X-ray structure analysis, spectral data and elemental analyses.

References

1 I. Kawamoto, T. Hata, Y. Kishida and C. Tamura, *Tetrahedron Lett.*, 1972, 1611.
2 I. Kawamoto, T. Hata, Y. Kishida and C. Tamura, *Tetrahedron Lett.*, 1971, 2417.
3 I. Kawamoto, Y. Sugimura and Y. Kishida, *Tetrahedron Lett.*, 1973, 877.
4 I. Kawamoto, Y. Sugimura, N. Soma and Y. Kishida, *Chem. Lett.*, 1972, 931.
5 T. Takayasu and M. Nitta, *J. Chem. Soc., Perkin Trans. 1*, 1997, 3255.
6 J. Emsley and D. Hall, *The chemistry of phosphorus*, Harper and Row Publishers, London, New York, Hagers town and San Francisco, 1976, pp. 82 and 83.
7 M. Nitta and S. Naya, *J. Chem. Res. (S)*, 1998, 522; M. Nitta and S. Naya, *J. Chem. Res. (M)*, 1998, 2363.
8 H. Yamamoto, M. Ohnuma and M. Nitta, *J. Chem. Res. (S)*, 1999, 173; H. Yamamoto, M. Ohnuma and M. Nitta, *J. Chem. Res. (M)*, 1999, 901.
9 N. Soma and I. Kawamoto, *Chem. Abstr.*, 1972, **76**, 59751t.
10 H. Bestmann and K. Roth, *Angew. Chem., Int. Ed. Engl.*, 1981, **20**, 575.
11 S. Ito, A. Kakehi, K. Okada and I. Shibazaki, *Heterocycles*, 2001, **54**, 237.
12 D. W. J. Cruikshank, *Acta Crystallogr.*, 1964, **17**, 671.
13 R. Francke, W. S. Sheldrick and G.-V. Röschenthaler, *Chem. Ber.*, 1989, **122**, 301.
14 G. Speier, Z. Tyeklar, V. Fülöp and L. Parkanyi, *Chem. Ber.*, 1988, **121**, 1685.
15 A. Bondi, *J. Phys. Chem.*, 1964, **68**, 441.
16 A. Krebs and B. Schrader, *Justus Liebigs Ann. Chem.*, 1967, **709**, 46.
17 M. J. Barrow, O. S. Mills and G. Filippini, *J. Chem. Soc., Chem. Commun.*, 1973, 66.
18 R. F. C. Brown and F. W. Eastwood, *J. Org. Chem.*, 1981, **46**, 4588.
19 R. M. Silverstein, G. C. Bassleer and T. C. Morrill, *Spectroscopic identification of organic compounds*, John Wiley & Sons, Inc., 1911, pp. 121 and 122.
20 G. Jones, R. K. Jones and M. J. Robinson, *J. Chem. Soc., Perkin Trans. 1*, 1973, 968; G. Jones and J. Robinson, *J. Chem. Soc., Perkin Trans. 1*, 1977, 505.
21 M. J. S. Dewar, E. G. Zoebisch, E. F. Healy and J. J. P. Stewart, *J. Am. Chem. Soc.*, 1985, **109**, 3902; M. J. S. Dewar and E. G. Zoebisch, *THEOCHEM*, 1988, **180**, 1.
22 A. Altomare, M. C. Burla, M. Camalli, M. Cascarano, C. Giacovazzo, A. Guagliardi and G. Polidori, *J. Appl. Crystallogr.*, 1994, **27**, 435.